Phase Rearrangement in Two-Stage Emulsion Polymers of Butyl Acrylate and Styrene: Mechanical Properties

KEVIN M. O'CONNOR and SHENG-LIANG TSAUR, *Corporate Research Division, Louis Laboratory, S. C. Johnson & Son, Inc., Racine, Wisconsin 53403*

Synopsis

The mechanical and thermal properties of films from a series of two-stage emulsion polymers were investigated. The emulsion polymers were made by polymerizng styrene in the presence of a preformed poly(butyl acrylate-co-divinyl benzene) seed latex. The effects of seed particle size, seed particle crosslinking via the amount of divinyl benzene, styrene/butyl acrylate ratio, and thermal history on the film properties were studied. Latex particles were characterized by light scattering and film formation behavior. Dried films were characterized by differential scanning calorimetry, dynamic mechanical analysis, and stress-strain behavior. Although evidence was obtained for nearly complete phase separation between the polystyrene (PS) and poly(butyl acrylate) (PBA) phases, the site of styrene polymerization and thus the PS phase morphology is influenced by seed particle size, seed crosslinking, and S/BA ratio. The morphology of as-dried films consists of finely dispersed PS domains in a continuous PBA matrix. Thermal annealing above the PS T_g causes coalescence of the PS domains, resulting in significantly improved mechanical properties. The extent of PS phase coalescence is also influenced by the level of seed crosslinking.

INTRODUCTION

In a multistage emulsion polymerization, the monomer feed composition is changed in a stage-wise manner during the polymerization. During each stage, the polymer being formed on or within the growing latex particle has a composition determined by the monomer feed used in that stage. Multistage processes provide a means for the controlled production of heterogeneous, structured latex particles exhibiting a wide variety of particle morphologies. As a result, films formed from these particles can exhibit more desirable physical properties than materials simply blended mechanically from the same polymer components. A successful commercial example is that of ABS polymers in which heterogeneous emulsion particles are prepared by polymerizing a styrene/acrylonitrile mixture in the presence of a polybutadiene latex.[1]

A complete understanding of the particle morphologies which develop requires consideration of a number of factors. The site of polymer formation depends on the relative hydrophobicity of monomers and already formed polymers and the solubility of monomers in the latex particle.[2] The degree of phase separation within the heterogeneous particle is determined by the miscibility or compatibility of different polymers, the mobility of each polymeric component, possible grafting reactions between growing chains and preformed polymer from a previous stage, and the thermal history of the emulsion.[2] When feed for a stage is a mixture of comonomers, one may

Journal of Applied Polymer Science, Vol. 33, 2007–2027 (1987)
 CCC 0021-8995/87/062007-21$04.00

encounter compositional heterogeneity as a function of conversion.[3,4] Phase separation within the particles can result from extreme compositional heterogeneity. In addition, process variables can influence particle morphologies. These include the method of monomer addition (i.e., batch, semibatch, power-feed, etc.),[5-7] initiator type,[8] and whether the stages are polymerized sequentially or a preformed latex is used as the source of seed particles.[9]

Over the past 20 years, the heterogeneous nature of multistage latex particles has been studied extensively by transmission electron microscopy,[5,6,8,10-13] emulsifier adsorption behavior,[14] analysis of surface functionality,[4] particle swelling,[4,15] and light scattering.[16] Systematic studies have generally been conducted on two-stage latex polymers of styrene and acrylic or methacrylic acids and esters.

The physical properties of films have also been investigated as a means to ascertain the heterogeneous nature of the particles from which the films were formed. Techniques and methods applicable to polymer blends have been used successfully to characterize films from multistage latex polymers. When relating film properties to particle morphology, it is important to recognize that film properties can also depend on phenomena which occur as the particles coalesce into films. Film properties studied in the past include optical clarity,[17] film-forming ability,[11] dynamic mechanical response,[7,18-20] adhesive properties,[21] stress-strain behavior,[17] and glass transition temperature.[11]

In this paper, we report on the mechanical properties of films from a two-stage latex polymer. The system chosen consists of a crosslinked poly(butyl acrylate) seed particle formed in the first stage of polymerization and polystyrene formed in the second stage. This pair of monomers, polymerized in a two-stage manner, can be expected to yield films having properties which range from those of a reinforced rubber to those of a rubber-modified glass, depending on the relative amounts of each stage and the nature of the multiphase morphology. The variables of concern in this study were the monomer feed ratio, the seed particle size, the degree of crosslinking within the seed, and the thermal history of the as-dried films from the two-stage latex polymers. It will be shown that the film morphology and thus the mechanical properties are sensitive to each of these variables. This paper will focus on the effect of seed crosslinking on film morphology and the effect of thermally induced phase rearrangment on mechanical properties.

EXPERIMENTAL

Materials

Butyl acrylate (BA) and styrene (S) monomers were technical grade, supplied by Monsanto Company. Sodium dodecyl sulfate (SDS) and potassium persulfate ($K_2S_2O_8$) were obtained from Aldrich Chemical. Divinyl benzene (DVB) was obtained from Monomer-Polymer and Dajac Labs, Inc. Filtered, deionized water (DIW) was used in all aspects of the synthesis.

Emulsion Polymerization

The BA seed particles were made by first purging all components under N_2 for 10 minutes. The SDS and DIW were charged to a 3-necked glass flask,

TABLE I
Seed Latex Polymerization

Sample designation	BA-0	BA-2	BA-5	BA-5L	BA-10
BA (g)	112	112	112	112	112
DVB (g)	0	2.27	6.68	6.68	11.36
$K_2S_2O_8$ (g)	0.50	0.50	0.50	0.50	0.50
SDS (g)	0.376	0.376	0.374	0.112	0.374
DIW (mL)	260	260	260	260	260
Temperature (°C)	75	75	75	75	75
Reaction time (h)	4	4	4	4	4
% Solids	29	29	29	23	31

followed by 10% of the BA/DVB mixture. The reaction vessel was then placed in an oil bath at 75°C and the mixture was stirred. The $K_2S_2O_8$ solution was added. After 5 min, the remainder of the BA/DVB mixture was added over the course of 2 h under N_2 atmosphere. The reaction was then held at 75°C for an additional 2 h. The reactions used for the various seed latex particles are shown in Table I.

Two-stage latex polymers were prepared by charging the prepurged seed latex, DIW, $K_2S_2O_8$, and SDS (if used) to a 3-necked glass flask. One half of the styrene was precharged to the flask and the mixture stirred for 10 min under N_2. The flask was then placed in an oil bath at 75°C and held for 5 min. The remainder of the styrene was added dropwise over 1 h. The reaction was held at 75°C for an additional 3 h. The reactions used in the two-stage polymerizations are summarized in Table II.

Gas chromatography was used to assess the levels of residual BA and styrene in the two-stage latex polymers. In all cases, residual BA was less than 0.1% and residual styrene less than 1.2%.

Particle Size Determination

Latex particle size was determined by dynamic laser light scattering using a Brookhaven digital correlator, Model BI2030. The particle diameter and polydispersity were obtained from analysis of the temporal correlation function of the scattered light. Data were treated in the standard manner for polydisperse systems.[22] The particle diameter D obtained from this method is

TABLE II
Two-Stage Latex Polymerization

Sample designation Seed latex type	SBA-0 BA-0	SBA-2 BA-2	SBA-5 BA-5	80SBA-5 BA-5	SBA-5L BA-5L	SBA-10 BA-10
Seed Latex (g)	100	99.7	100	60	100	94.5
S (g)	27.4	27.4	27.4	70.3	21.9	27.4
$K_2S_2O_8$ (g)	0.2	0.2	0.2	0.2	0.2	0.2
SDS (g)	0	0	0	0.05	0.05	0
DIW (mL)	58.2	58.5	30.4	24.0	24.3	63.7
Temperature (°C)	75	75	70	70	70	75
Reaction time (h)	4	4	4	4	4	4

equal to $\langle D^6 \rangle / \langle D^5 \rangle$ and the polydispersity is given by $\langle D^6 \rangle \langle D^4 \rangle / \langle D^5 \rangle^2 - 1$, where $\langle D^\eta \rangle$ is the η-th moment of the particle size distribution. A monodisperse latex has a polydispersity of zero by this definition.

Differential Scanning Calorimetry

Differential scanning calorimetry (DSC) was performed using a DuPont 910 DSC module attached to a DuPont 1090B Thermal Analyzer. Sample size was 5 to 10 mg of the dried latex. A heating rate of 20°C/min was used in all cases.

High purity water and indium samples were run to correct for temperature offset in the instrument. The glass transition temperature (T_g) was defined as the temperature at the midpoint of the change in heat capacity.

Dynamic Mechanical Analysis

The dynamic mechanical behavior of films cast from the two-stage emulsions was investigated using a DuPont 982 DMA module attached to the DuPont 1090B Thermal Analyzer. Films of 0.5 mm thickness were cast on glass plates and dried at least two weeks at ambient conditions. For emulsions which did not form continuous films when dried at room temperature, films were made by pressing the dried fragments at 160°C for 10 min in a Carver laboratory press. Films were stored under vacuum prior to use. Specimen strips were clamped horizontally in the DMA, and the length-to-thickness ratio was maintained at approximately 1.0. In this geometry, the deformation is predominantly shear and the observed shear moduli are insensitive to the value chosen for Poisson's ratio. The oscillation amplitude was 0.1 mm. All dynamic mechanical data were obtained at a heating rate of 2°C/min under a nitrogen atmosphere.

Tensile Testing

Tensile testing was performed using an Instron Model 1123 testing machine. Dogbone-shaped specimens having a gauge section 25 mm long and 7 mm wide were cut from 0.5-mm thick films prepared as for dynamic mechanical analysis. Tests were conducted at an extension rate of 12.7 mm/min at 20°C and 50% relative humidity (RH).

Thermal Annealing

In the sections to follow, references were made to various thermal annealing treatments. In all cases, annealing was performed under a nitrogen atmosphere. Samples for DSC and DMA were annealed in their respective test geometries. Samples for Instron testing were annealed as films and then cut to the desired shape. A standard annealing treatment of one hour of 140°C was used unless noted otherwise.

RESULTS AND DISCUSSION

In Tables I and II and in the discussion to follow, samples are identified using the following system. Poly(butyl acrylate) seed latices are designated

TABLE III
Latex Particle Size

Sample Designation	Particle diameter (nm)	Polydispersity
BA-0 (seed)	100.6 ± 0.8	0.03
SBA-0	121.8 ± 1.1	0.02
BA-2 (seed)	90.3 ± 1.2	0.03
SBA-2	118.0 ± 2.5	0.06
BA-5 (seed)	73.6 ± 1.0	0.05
SBA-5	130.0 ± 1.7	0.12
80SBA-5	136.0 ± 1.4	.09
BA-5L (seed)	141.6 ± 1.9	< 0.01
SBA-5L	181.0 ± 1.4	0.08
BA-10 (seed)	118.6 ± 0.4	0.07
SBA-10	123.6 ± 2.8	0.07

"BA" followed by a number representing the mol% of crosslinking monomer (DVB), e.g., a designation of "BA-5" indicates 5 mol% DVB in the seed. A two-stage latex polymer formed by polymerizing styrene in the presence of this seed is designated "SBA-5." All except one of the two-stage polymers investigated in this study had an approximately 1 : 1 ratio of styrene to butyl acrylate based on weight; the sample designated 80SBA-5 was 80% styrene and 20% butyl acrylate. Finally, two butyl acrylate seeds were prepared at 5% DVB with widely different particle sizes (see Table III). The larger of these seeds is designated "BA-5L."

Particle Size

The measured particle diameters and their associated polydispersities are summarized in Table III. The particles are reasonably monodispersed, with all seeds and all two-stage particles except one having polydispersity indices less than 0.1. Using the ratio of styrene to seed latex and the density of polystyrene, one can predict the increase in particle diameter upon conversion of seed latex to two-stage latex, assuming no increase in particle population and no particle coagulation. The calculated diameter is $D_{\text{two-stage}} = 1.27\ D_{\text{seed}}$ for all samples except 80SBA-5, for which $D_{\text{two-stage}} = 1.71\ D_{\text{seed}}$. The particle diameters in Table III are in general agreement with prediction. Anomalous results were observed for SBA-5 and SBA-10, for which $D_{\text{two-stage}}/D_{\text{seed}}$ was 1.77 and 1.04, respectively. It is noted that SBA-5 exhibits the highest polydispersity of the two-stage particles, possibly due to a certain amount of particle coagulation which would simultaneously increase the apparent particle diameter and the polydispersity. No explanation is apparent for SBA-10, which exhibits a diameter and polydispersity nearly equal to the seed from which it was made. It is unlikely that the added styrene formed a separate particle population since no additional surfactant was added in the second stage.

Film Formation

The ability of a polymer latex to form a continuous film with mechanical integrity depends on the viscoelastic relaxation of the particle under the forces

exerted by surface tension[23] and the interpenetration of molecules across particle–particle boundaries. Both factors are related to the glass transition temperature (T_g) of the polymer, and in particular to the T_g of the molecular species present in the surface layers of the particle. Butyl acrylate/styrene two-stage latex polymers represent a case in which one component (BA) has a T_g about 70°C below room temperature while the other component (S) has a T_g about 80°C above room temperature. Thus, the ability of these latices to form films yields some information about the composition of the particle surfaces. Samples SBA-0, SBA-2, and SBA-5 all formed continuous films, with the optical clarity decreasing with increasing level of crosslinking. Sample SBA-10, with a higher level of crosslinking, did not form a continuous film at room temperature but rather dried into a brittle, white solid. Sample SBA-5L, which differed from SBA-5 only in that a larger seed particle was used, formed a film which was largely continuous but cracked into fragments having sizes on the order of a centimeter. Sample 80SBA-5, having four times more styrene per unit of seed latex than SBA-5, formed a film which fragmented into millimeter-sized pieces.

The film-forming ability of these latices can be interpreted in terms of the possible morphologies of the particles. Samples SBA-0, SBA-2, and SBA-5 have surface layers with T_g's below room temperature, indicating a composition rich in PBA. Conversely, samples SBA-5L, 80SBA-5, and SBA-10 have surfaces rich in PS. It is not possible to extract quantitative information about particle morphology from the film-forming behavior at room temperature. However, several qualitative conclusions can be drawn. Under the polymerization conditions used in this study, the majority of the styrene polymerizes inside seed particles having DVB levels from 0 to 5 mol%. At 10% DVB, a significant amount of styrene polymerizes on or very near the seed particle surface. Similarly, the effect of increased seed particle size or increased styrene level is to increase the amount of polystyrene formed on or near the seed particle surface. Min and co-workers[6] used thin-layer chromatographic techniques to confirm the presence of graft copolymer species in BA/S two-stage polymers. At reaction temperatures similar to those in this work, they found that the fraction of PBA existing as graft copolymer depended on the method of styrene addition. For equilibrium preswelling of the PBA seed particles by styrene, 16% of the PBA was grafted to PS. For dropwise addition of styrene to the seed latex, 7.8% was grafted. Our method of styrene addition is essentially a combination of preswelling and dropwise addition, and grafting levels in the range of 8 to 16% can be expected. We are currently investigating use of chromatographic and spectroscopic techniques to determine if the level of grafting is influenced by seed crosslinking.

Differential Scanning Calorimetry

Differential scanning calorimetry (DSC) is an important method for the evaluation of miscibility between components of polymer blends.[24] In the absence of miscibility, a blend of two amorphous polymers exhibits two glass transitions with the transition temperatures coinciding with the T_g's of the pure components. In cases of particle miscibility, the T_g's, although distinct, are shifted and sometimes broadened toward each other. For miscible blends,

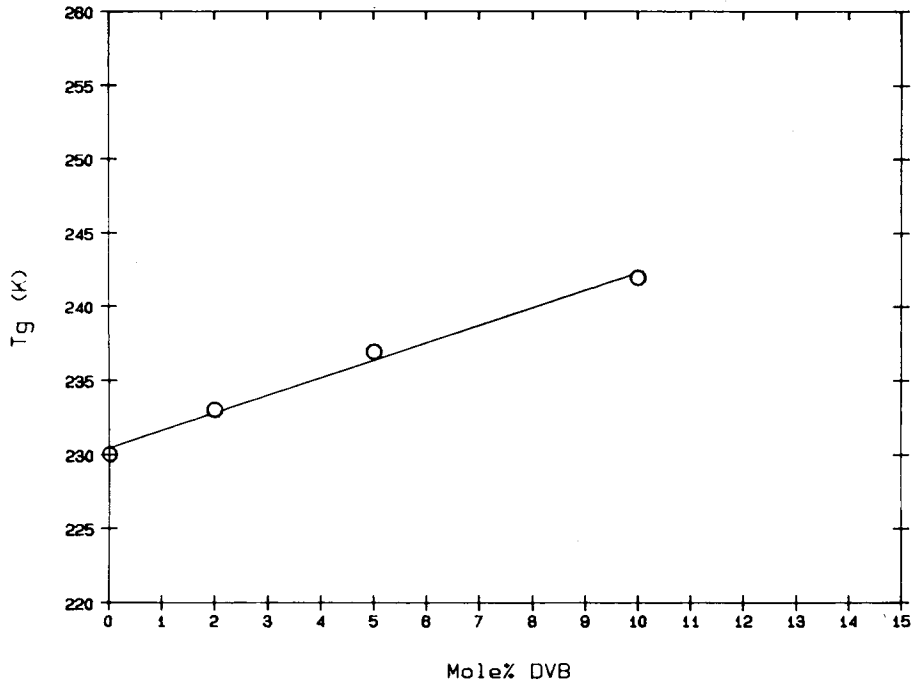

Fig. 1. Glass transition temperature of dried films of BA seed latices versus mol% divinyl benzene.

a single T_g is observed at a temperature between the component T_g's determined by the relative amounts of each component. This latter behavior represents a valid definition of polymer-polymer miscibility.[24]

DSC was used to characterize both the BA seeds and the BA/S two-stage polymers. Figure 1 shows the seed T_g as a function of the mol% DVB in the seed. As expected from chain mobility considerations, the T_g increases with increasing level of crosslinking. A DSC trace for the SBA-0 two-stage polymer is shown in Figure 2. The T_g's of PBA and PS are evident at approximately -43 and 94°C, respectively. These transitions occur at temperatures which closely coincide with those of pure PBA and PS. Furthermore, the transition temperatures are not sensitive to thermal annealing. The DSC traces for as-dried and annealed samples (Fig. 2) differ only in the endothermic cap associated with the polystyrene T_g for the as-dried sample. The disappearance of this cap upon rescanning is a thermal history effect observed in polymer glasses[25] which is not related to interactions between the PS and PBA phases. Behavior similar to Figure 2 was observed for all the two-stage polymers investigated; that is, the T_g of the PBA was determined by the seed crosslinking level and was minimally affected by the second-stage polymerization of styrene or by thermal annealing. Similarly, the T_g of the PS was not affected by thermal annealing.

The results of the DSC investigations for all samples show that, within the limits of detection via calorimetry, the PBA and PS exist as two separate phases without extensive phase mixing or interphase regions. However, in the

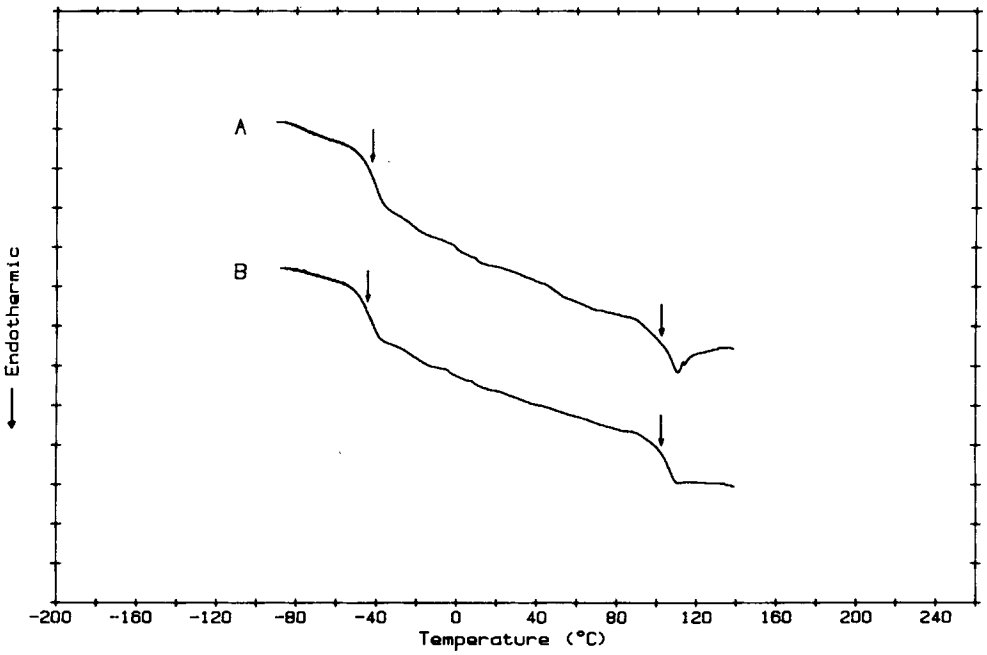

Fig. 2. DSC traces of films from two-stage latex SBA-0 (0% DVB). Curve A: as-dried. Curve B: after annealing 1 h at 140°C.

following sections it will be shown that the phase morphology is quite sensitive to seed crosslinking, seed particle size, and seed/styrene ratio.

Effect of Seed Crosslinking

In this section, results are presented on the mechanical properties of films as a function of the extent of crosslinking within the seed particle. Dynamic mechanical analysis (DMA) is a technique often used to characterize phase behavior in polymer blends. As with DSC, the behavior of mechanical relaxations associated with T_g provides an assessment of miscibility.[26] A highly phase-separated blend exhibits maxima in the mechanical loss at temperatures identical to those of the pure components, whereas a miscible blend exhibits a single loss peak at an intermediate temperature determined by the relative amounts of each component. Similarly, the storage component of the dynamic modulus exhibits an abrupt decrease in the region of each T_g in a phase-separated blend. Figure 3(a) shows the shear storage modulus G' as a function of temperature for films of sample SBA-0. For the sample annealed above the T_g of PS, decreases in G' at approximately -40 and 105°C are associated with the T_g's of PBA and PS, respectively. For the as-dried sample, the PBA transition is evident, as is a broad decrease in G' over the temperature range -10 to 60°C. No evidence of a PS transition is seen in the region of 100°C; in fact, the specimen is too compliant above 60°C to participate in the mechanical resonance set up by the instrument. A profound increase in G' above T_g of the PBA is observed upon annealing. For example, the storage modulus at 40°C increases by more than an order of magnitude after annealing. Figure

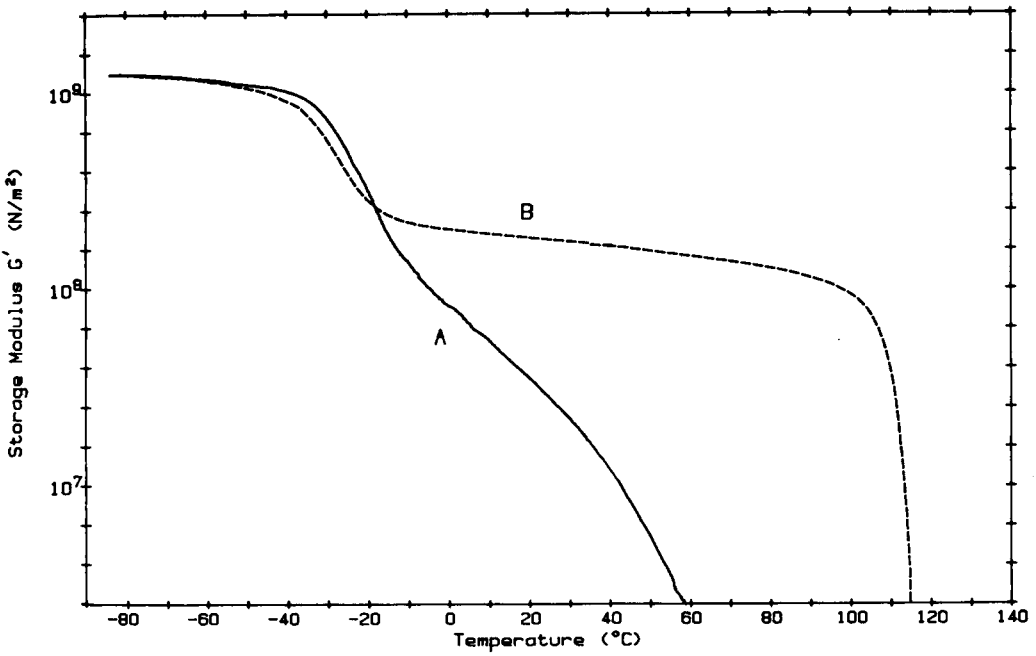

Fig. 3(a). Storage modulus G' versus temperature for films from two-stage latex SBA-0 (0% DVB). Curve A: as-dried. Curve B: after annealing 1 h at 140°C.

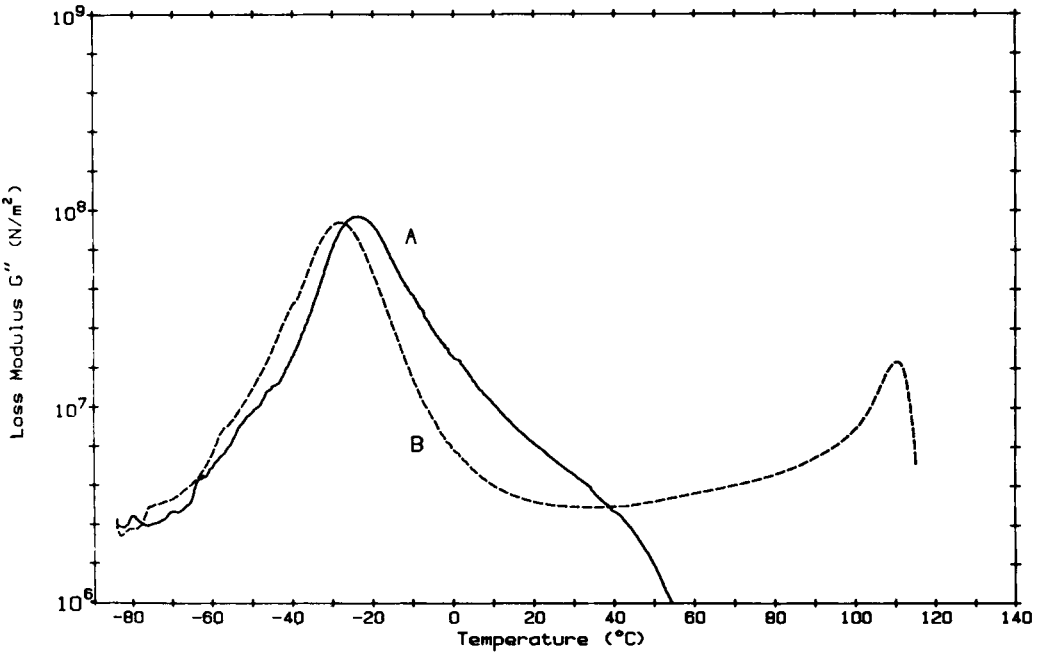

Fig. 3(b). Loss modulus G'' versus temperature for films from two-stage latex SBA-0 (0% DVB). Curve A: as-dried. Curve B: after annealing 1 h at 140°C.

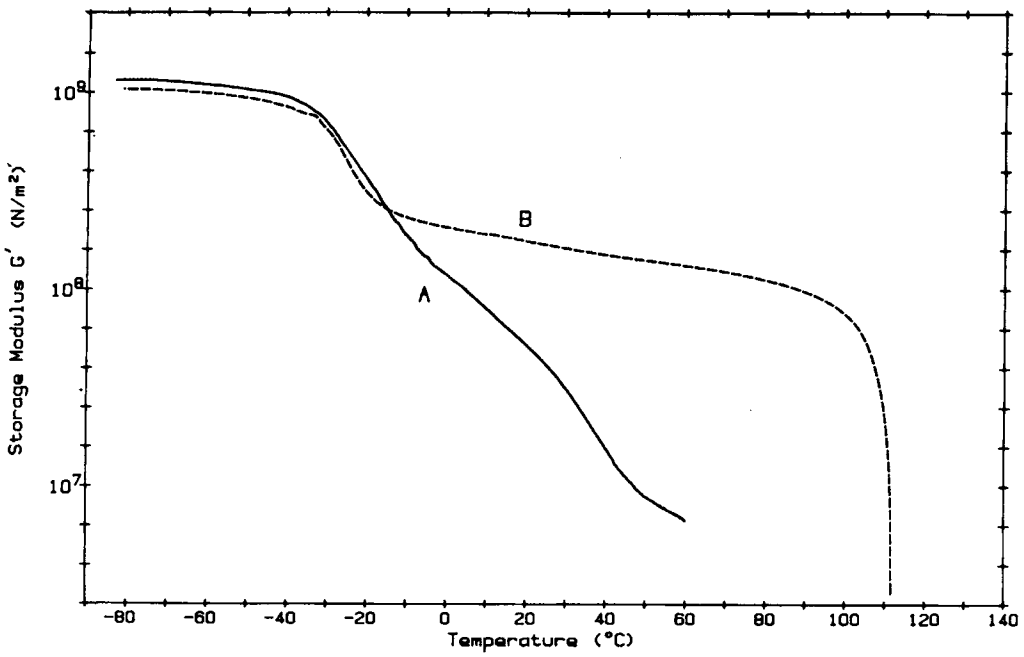

Fig. 4(a). Storage modulus G' versus temperature for films from two-stage latex SBA-2 (2% DVB). Curve A: as-dried. Curve B: after annealing 1 h at 140°C.

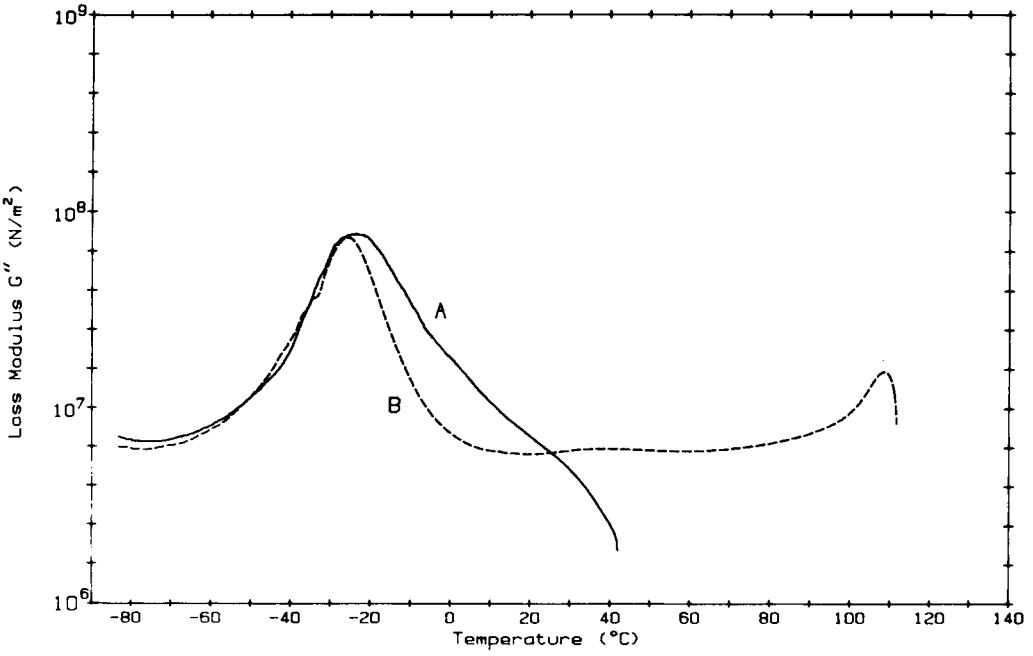

Fig. 4(b). Loss modulus G'' versus temperature for films from two-stage latex SBA-2 (2% DVB). Curve A: as-dried. Curve B: after annealing 1 h at 140°C.

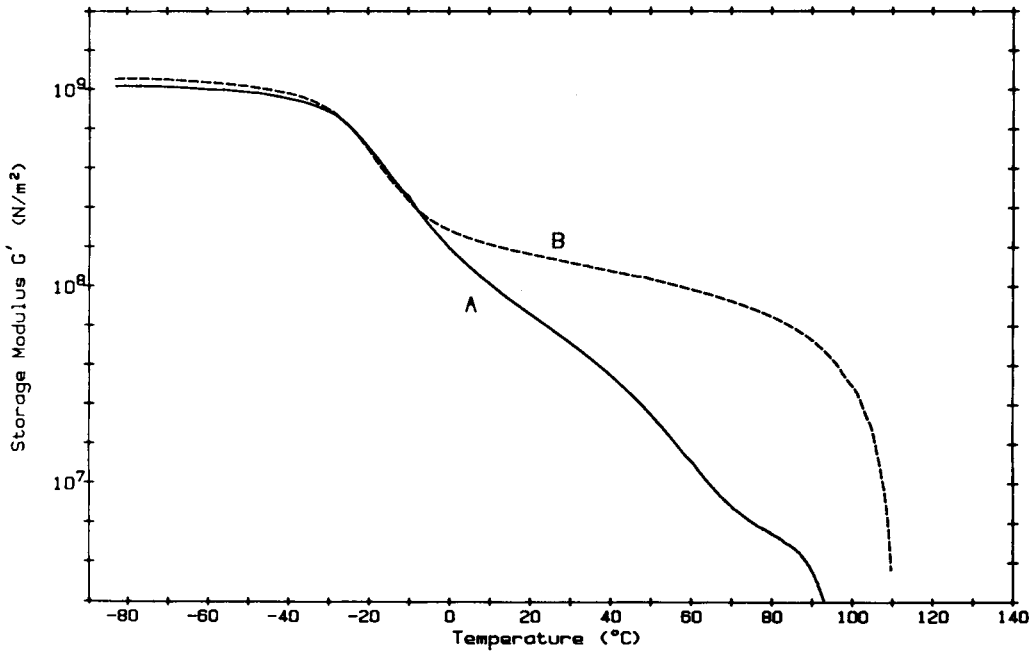

Fig. 5(a). Storage modulus G' versus temperature for films from two-stage latex SBA-5 (5% DVB). Curve A: as-dried. Curve B: annealed 1 h at 140°C.

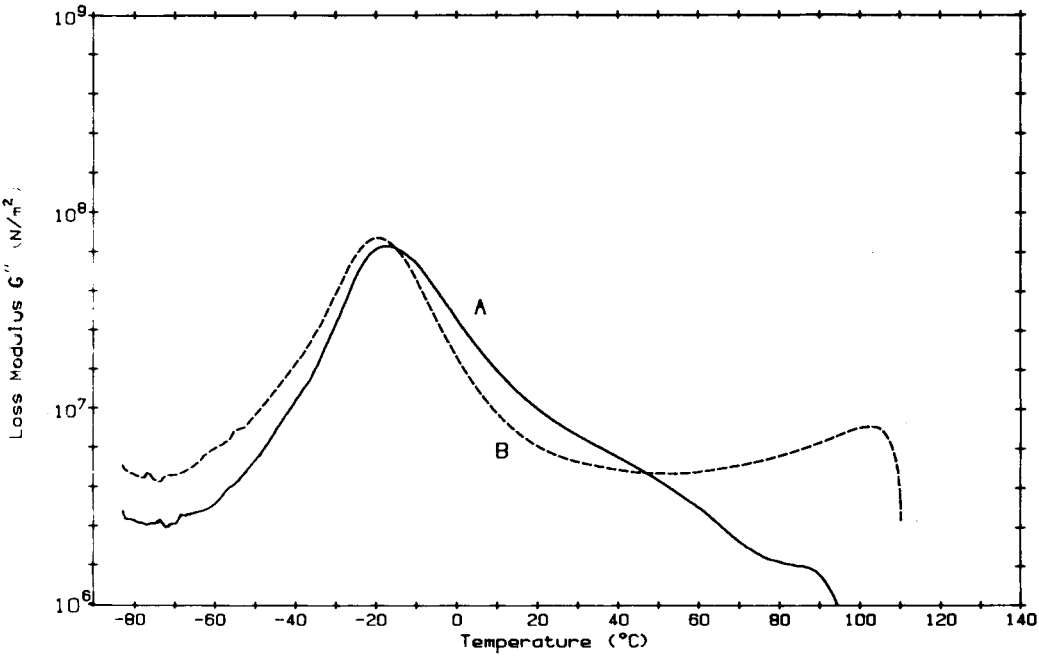

Fig. 5(b). Loss modulus G'' versus temperature for films for two-stage latex SBA-5 (5% DVB). Curve A: as-dried. Curve B: after annealing 1 h at 140°C.

3(b) shows the shear loss modulus G'' as a function of temperature for the same samples as in Figure 3(a). In the annealed state, two mechanical loss peaks are evident, corresponding to phase-separated PBA and PS. In the as-dried state, only the PBA peak is clearly distinguishable. The apparent broadening of this peak on the high temperature side is attributed to a broad, weak relaxation in the region of 20 to 40°C. The G'' peak associated with PBA shifts by 5°C to lower temperatures upon annealing. Lack of mechanical resonance above 60°C prohibits the mechanical detection of a pure PS phase in the as-dried state. Figures 4(a) and (b) show G' and G'', respectively, for sample SBA-2 (2% DVB) in the as-dried and annealed states. Qualitatively, the behavior is similar to SBA-0, but significant differences are observed. In the as-dried state, G' of SBA-2 is higher than that of SBA-0 at temperatures above T_g of the PBA phase. However, G' of SBA-2 in this temperature range increases by a smaller factor after annealing than does G' for SBA-0. This effect is partly attributed to G' of annealed SBA-2 decreasing faster with temperatures at $T > 0$°C than G' of annealed SBA-0. In the as-dried state, a hint of a plateau in G' is evident at 50–60°C. The effect of annealing on G'' [Fig. 4(b)] is to narrow the PBA loss peak on the high temperature side and shift its maximum 4°C lower. A distinct PS loss peak is also seen after annealing. The behavior of G'' for SBA-2 before and after annealing is similar to that of SBA-0.

The effects of increased seed crosslinking are more pronounced for sample SBA-5 (5% DVB), for which G' and G'' are shown in Figures 5(a) and (b), respectively. In the as-dried state above the T_g of PBA, G' is higher than for 0 and 2% DVB and the difference in G' between as-dried and annealed samples is smaller. A minor plateau in G' is observed near 80°C. As with the samples having lower levels of crosslinking, the effect of annealing is to narrow and shift to lower temperature (by 3°C) the PBA loss peak. The effect of annealing on G'' is shown in Figure 5(b). The dynamic mechanical behavior of SBA-10 (10% DVB in the seed) in the as-dried state was not investigated due to its inability to form continuous films under the same drying conditions used for the other samples.

The effect of seed crosslinking on the multiphase morphology of the as-dried samples is demonstrated in Figure 6, which shows $G'(T)$ for SBA-0, SBA-2, and SBA-5 in the as-dried state. As stated above, increased crosslinking in the seed results in higher values of G' above the PBA transition temperature and promotes the appearance of a weak plateau in G' which appears at about 80°C for 5% DVB.

The effect of seed crosslinking on the morphology of annealed samples is shown in Figure 7. Of particular interest are the magnitude and temperature sensitivity of G' above the PBA transition temperature. Increasing the DVB level in the seed results in lower values of G' in this temperature region (opposite to the behavior observed in as-dried samples) and increased slope of $\log G'$ versus T at temperatures intermediate to the PBA and PS transitions.

The results presented above indicate that the dynamic mechanical behavior, in contrast to DSC, is quite sensitive to seed crosslinking and thermal annealing. An explanation is possible based on morphological effects. The dynamic mechanical response of a phase-separated blend, in which the components differ widely in T_g, is largely determined by the relative volume

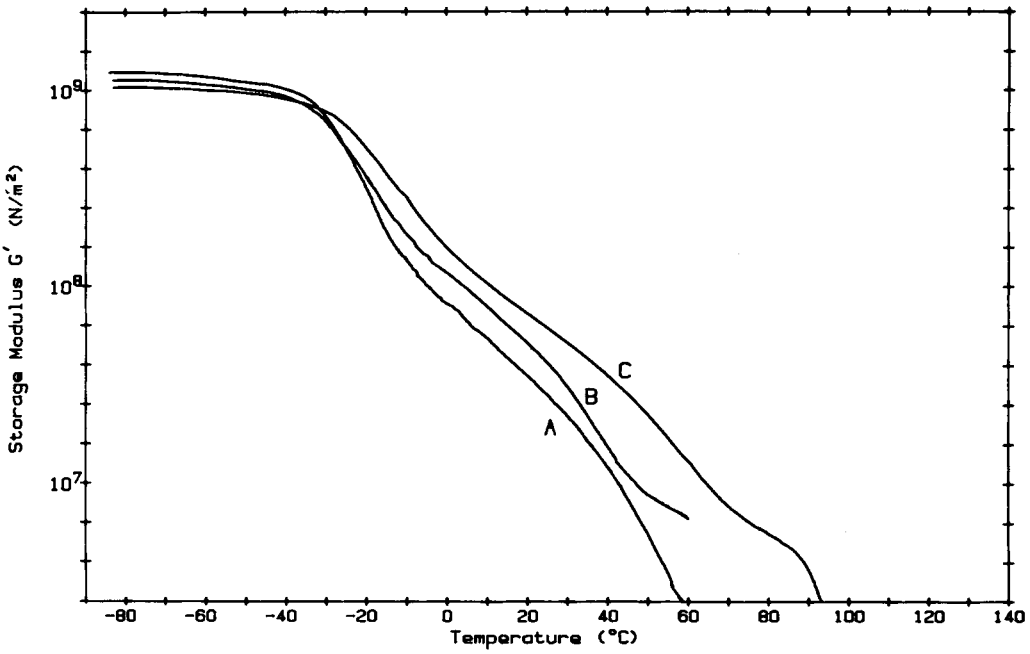

Fig. 6. Effect of seed crosslinking on G' of as-dried films. Curve A: SBA-0 (0% DVB). Curve B: SBA-2 (2% DVB). Curve C: SBA-5 (5% DVB).

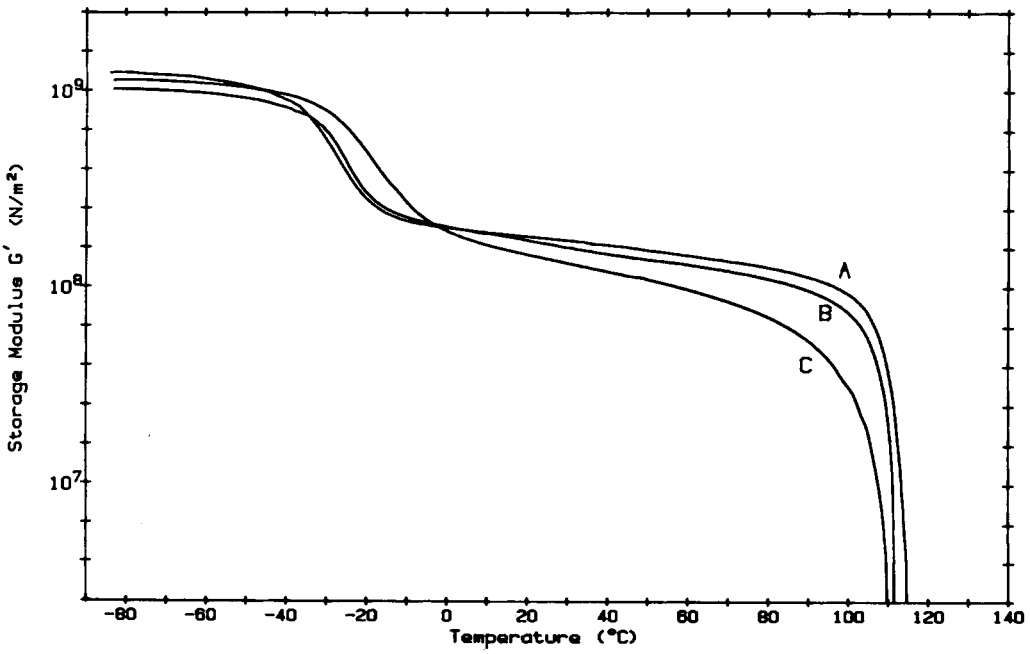

Fig. 7. Effect of seed crosslinking on G' of films annealed 1 hour at 140°C. Curve A: SBA-0 (0% DVB). Curve B: SBA-2 (2% DVB). Curve C: SBA-5 (5% DVB).

fractions of each phase, the identity and characteristic size of the dispersed and continuous phases, the molecular weight of the phases, and the degree of adhesion between the phases.[26] The DSC results presented in Figure 2 indicate the lack of mixing between the PBA and PS phases. On this basis, the samples are judged to be well phase-separated in both the as-dried and annealed states. The nominal volume fractions of each phase are thus determined by the 1 : 1 ratio of styrene monomer to seed particle, and are the same for all samples. The differences observed in the dynamic mechanical behavior can be attributed to differences in the mechanically effective volume fraction of PS within the PBA matrix.

By virtue of the greater hydrophobicity of styrene relative to the PBA seed particle, the majority of the styrene is expected to diffuse into the seed and subsequently polymerize in the interior of the seed particle rather than on the surface. This is particularly true in view of the precharge, at room temperature, of half the styrene to the seed latex. Styrene monomer, being miscible with PBA, should be uniformly distributed throughout the seed particle except possibly at the particle surface. For example, the time required to achieve an equilibrium concentration change for a small molecule being sorbed by a spherical particle is estimated as 20 times the sorption halftime[27]:

$$t_{eq} = (20)7.66 \times 10^{-3} D^2/D_s$$

where D is the diameter of the particle and D_s is the diffusion coefficient of the small molecule in the particle. For a particle diameter of 100 nm, equilibrium uptake of styrene by the particle would occur in 10 min if D exceeds 2.6×10^{-14} cm^2/s. Values of D_s for organic liquids in polymers above T_g are on the order of 10^{-8} to 10^{-10} cm^2/s.[28] This calculation indicates that swelling of the seed particles by styrene monomer is rapid, and that a uniform distribution of the precharged styrene should exist within the seed particles.

Due to the incompatibility of PS and PBA, phase separation should occur within the seed particle as a result of the increasing chain length of PS during polymerization of the second stage. This is confirmed by the detection of the PS T_g, identical to the T_g of pure PS, via DSC for the as-dried samples. However, the degree of organization within the PS phase is a complicated function of the relative kinetics of chain growth and phase separation by diffusion. An additional consideration is that the polymerization temperature (70°C) is below the T_g of PS. Using the relation $T_g = T_{g\infty} - K/M_n$, where $T_{g\infty} = 100$°C and $K = 1.0 \times 10^5$,[29] one predicts that growing chains with $M_n > 3300$ would have little mobility at the 70°C reaction temperature because they are below their respective T_g's, resulting in the PS phase being formed as small domains with a low degree of interconnectivity. This argument is modified by the ability of styrene monomer to plasticizer polystyrene. As presented earlier in Figure 6, increased levels of crosslinking result in a more identifiable mechanically active phase above the PBA transition temperature in as-dried samples. The mechanical detection of this phase can be attributed to a larger PS domain size, a higher degree of connectivity within the PS phase, or both.

The dramatic changes in the dynamic mechanical response after annealing are attributed to a thermally induced coalescence of the PS phase. Above the

polystyrene T_g, sufficient molecular mobility exists to allow the PS phase to rearrange via self-diffusion into an equilibrium morphology which minimizes the interfacial surface energy between the PBA and PS phases. Because the volume fractions of the phases are nearly equal, the PS and PBA phases should be essentially co-continuous. Such a morphology results in the detection of a distinct PS damping peak and a modulus plateau between the PBA and PS transition temperatures. The level of seed crosslinking apparently influences the extent of coalescence within the PS phase. This can be seen in three ways. First, the change in G' between the as-dried and annealed states, at temperatures between the PBA and PS transitions, decreases with increasing seed crosslinking. Second, the magnitude of G', at temperatures between the PBA and PS transitions, decreases with increasing seed crosslinking. Third, the intensity of the G'' peak associated with the PS phase decreases with increasing seed crosslinking. These results are consistent with the idea that seed crosslinking limits the mobility of the PS phase and restricts the extent to which the PS phase coalesces during annealing.

Effect of Seed Particle Size

Seed latex samples BA-5 and BA-5L represent seed particles having identical DVB levels of 5% but having diameters of 73.6 and 141.6 nm, respectively. As discussed previously, the two-stage polymer SBA-5L was a marginal film-forming latex at room temperature. Large enough film fragments were obtained to permit DMA tests to be performed. Figure 8 compares G' for samples SBA-5 and SBA-5L in the as-dried state. The low modulus seen for

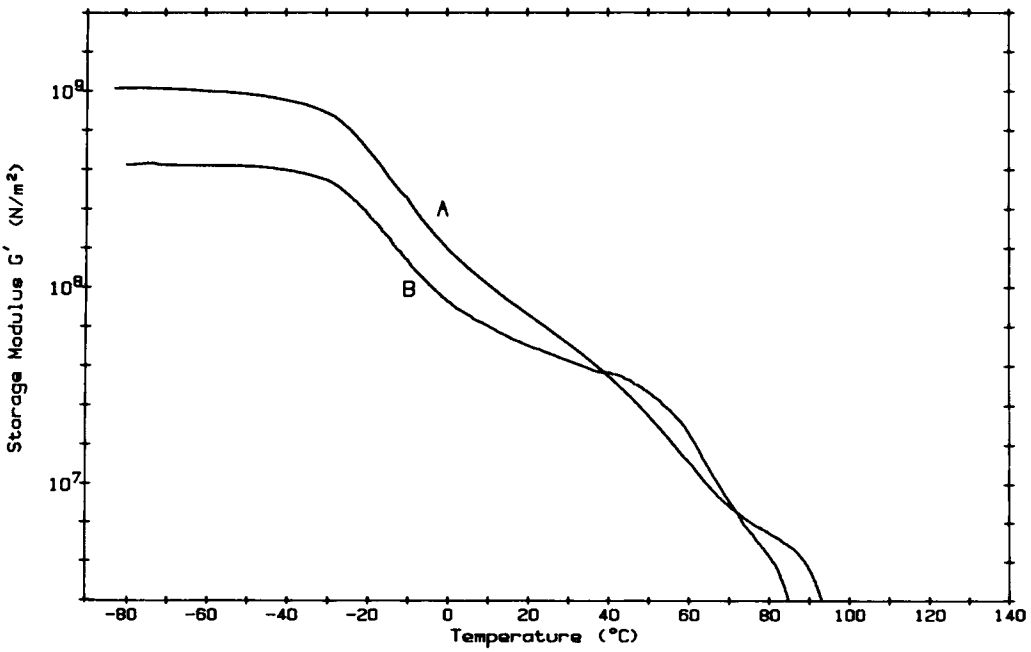

Fig. 8. Effect of seed particle size on G' of as-dried films. Curve A: SBA-5 (73.6 nm diameter). Curve B: SBA-5L (141.6 nm diameter).

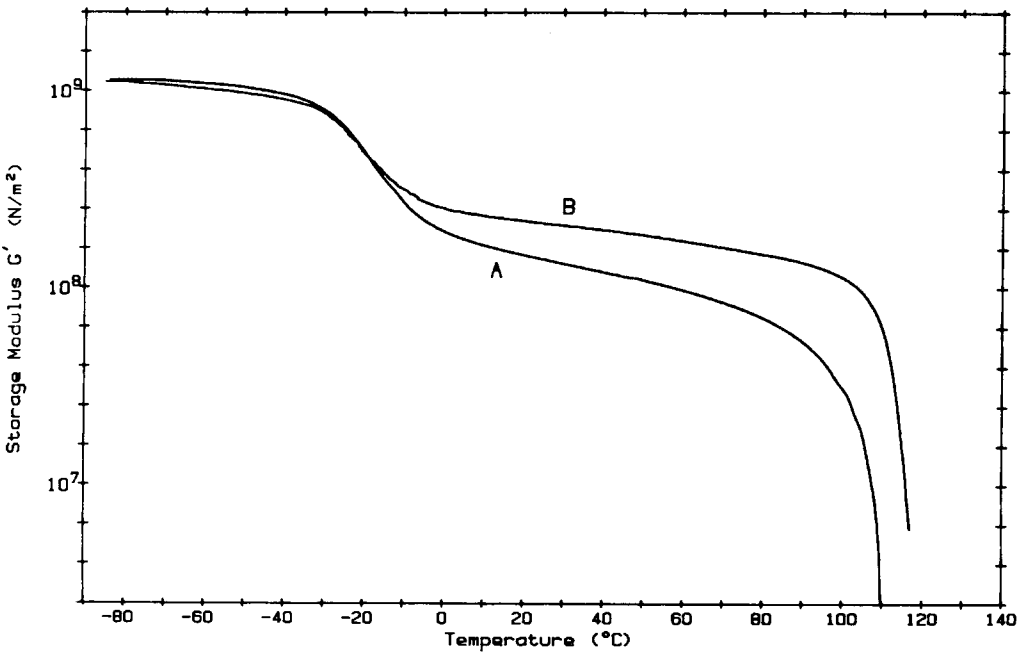

Fig. 9. Effect of seed particle size on G' of annealed films. Curve A: SBA-5 (73.6 nm diameter). Curve B: SBA-5L (141.6 nm diameter).

SBA-5L at low temperature is probably due to residual porosity in the poorly coalesced film. Although the absolute moduli cannot be compared for this reason, both SBA-5 and SBA-5L show evidence for a transition in the 50–60°C region in the as-dried stage. The plateau in G' at about 80°C for SBA-5 is not seen in SBA-5L. Annealing promotes further coalescence of SBA-5L and permits a direct comparison between the samples in the annealed state. Figure 9 shows samples SBA-5 and SBA-5L in the annealed state. The major effect of the larger seed particle is increase the magnitude of G' in the temperature region between the T_g's of PBA and PS. In the crosslinking study, this effect was attributed to more extensive coalescence of the PS phase; an identical argument applies in this case. The poor film-forming ability of the two-stage polymer using the larger seed is due to a more PS-rich surface layer. This effect may be due to the inability of the styrene monomer to swell the larger seed particle to an equilibrium level in the time prior to its polymerization, leading to a surface layer richer in PS for the larger seed. The relative abundance of PS at the particle surface leads to a more extensively coalesced PS phase in the annealed SBA-5L than in the annealed SBA-5.

Further insight into the phase coalescence phenomenon and the effect of seed particle size is available from the stress-strain behavior of the films. Figure 10 shows the stress-strain curves for as-dried SBA-5 and annealed SBA-5 and SBA-5L. In the as-dried state, the behavior of SBA-5 is that of a soft thermoplastic. Elongations of 150% are achieved with uniform drawing of the gauge section and without necking or stress-whitening up to the point of

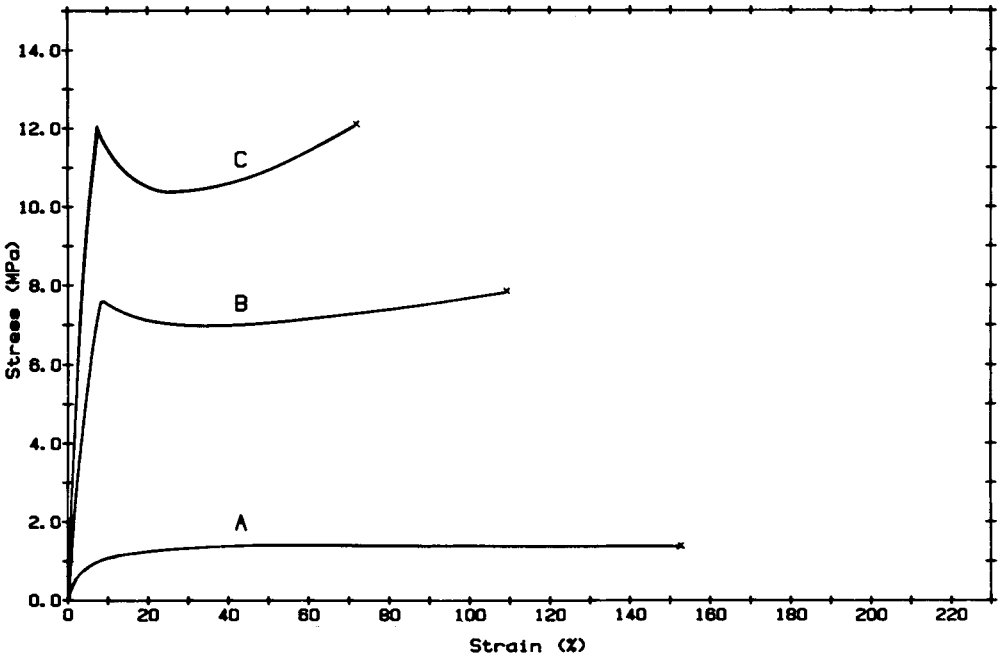

Fig. 10. Stress-strain curves for two-stage latex films. Curve A: SBA-5 as-dried. Curve B: SBA-5 annealed. Curve C: SBA-5L annealed.

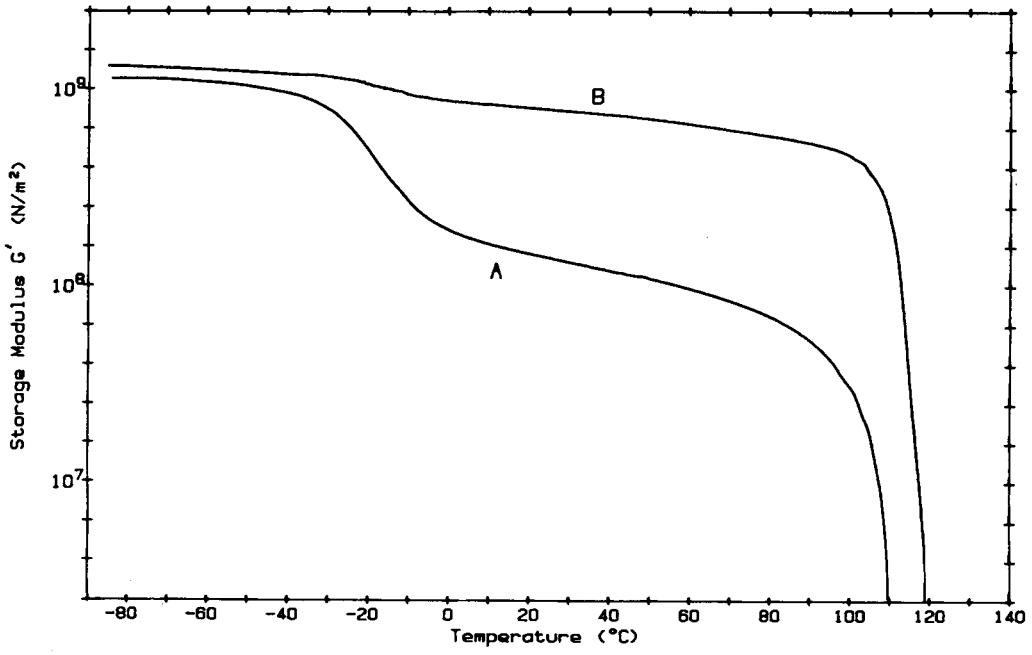

Fig. 11. Effect of styrene content on G' of annealed two-stage latex films. Curve A: SBA-5 (50% styrene). Curve B: 805BA-5 (80% styrene).

TABLE IV
Mechanical Properties

Sample designation	SBA-5 (AD[a])	SBA-5 (A[b])	SBA-5L (A)	80SBA-5 (A)
Tensile modulus (MPa)	37.0	177	262	700
Yield stress (MPa)	—	7.5	12.1	36.9
Yield strain (%)	—	7.7	7.0	6.7
Fracture stress (MPa)	1.3	7.9	12.1	34.5
Fracture strain (%)	150	109	71.2	11.5
Energy to fracture (J)	2.1	8.3	8.1	2.9

[a]AD = as-dried.
[b]A = annealed.

fracture. The stress-strain behavior of annealed SBA-5 is dramatically different, with higher modulus, fracture stress, and fracture energy, lower fracture strain, and the presence of a yield point. In this study, the fracture energy was defined simply as the area under the stress-strain curve up to the point of fracture. For annealed SBA-5, localized stress-whitening was observed in the specimen at the yield point, with the whitening spreading uniformly throughout the gauge section as the specimen was drawn to fracture. No localized necking was observed. The poorly-coalesced nature of sample SBA-5L prohibited the measurement of its stress-strain behavior. Data for annealed SBA-5L are also shown in Figure 10. Comparison with annealed SBA-5 indicates that the larger seed particle results in films having higher modulus, yield stress, and fracture stress, a more pronounced yield point, and lower fracture strain. The data of Figure 11 are consistent with the phase coalescence discussed earlier in relation to the dynamic mechanical results. The presence of a yield point is due to a certain degree of connectivity within the PS phase. The association of a yield point with interconnectivity within the PS phase has been made previously for phase-separated styrene-butadiene-styrene triblock copolymers.[30] The higher tensile modulus of SBA-5L is consistent with the higher dynamic shear modulus at room temperature observed in Figure 9. The stress-strain properties of various films are summarized in Table IV.

Effect of Styrene Content

The effect of styrene content on the mechanical properties was briefly studied using sample 80SBA-5 which uses the same seed particle as SBA-5 but has a 4 : 1 ratio of styrene to butyl acrylate rather than the 1 : 1 ratio used in SBA-5. Due to the high polystyrene level, film formation was poor for 80SBA-5 and no measurements were possible in the as-dried state. Figure 11 shows G' for annealed SBA-5 and 80SBA-5. In this case, both specimens were prepared by compression molding the dried latices for 10 min at 160°C. The behavior of the SBA-5 sample prepared in this manner was very similar to that of samples annealed in the standard way. As expected, the major effect of the increased PS content is to increase the intensity of the PS transition relative to the PBA transition, with a higher modulus plateau at intermediate

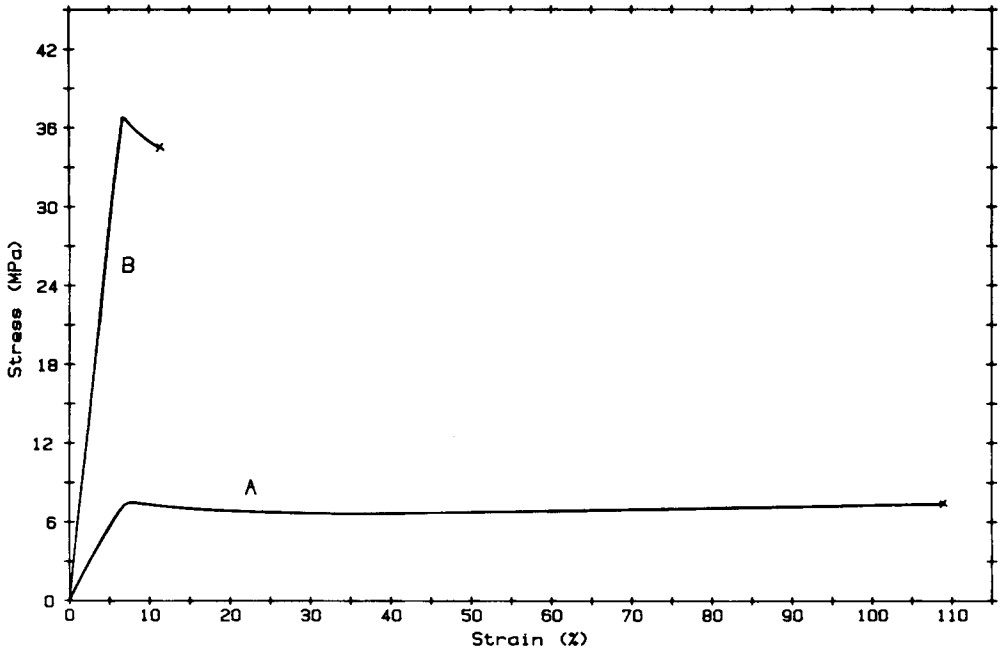

Fig. 12. Effect of styrene content on stress-strain behavior of annealed films. Curve A: SBA-5 (50% styrene). Curve B: 80SBA-5 (80% styrene).

temperatures. The stress-strain behavior of annealed SBA-5 and 80SBA-5 is shown in Figure 12. The increased level of PS results in much higher modulus, yield stress and fracture stress, and lower fracture strain and energy. These properties are summarized in Table IV. A yielding and stress-whitening phenomenon occurs in 80SBA-5 similar to annealed SBA-5 and SBA-5L, with all three samples exhibiting similar values of yield strain of approximately 7%. With the exception of its rather low fracture strain, the behavior of 80SBA-5 is similar to that of commercial rubber-modified polystyrenes.

SUMMARY

This paper has investigated the phase behavior of films from two-stage latex polymers based on butyl acrylate and styrene. Results from differential scanning calorimetry, dynamic mechanical analysis, tensile testing, and film formation studies were used to describe the phase morphology of the as-dried and annealed films. The as-dried morphology of 50:50 PBA/PS systems consisted of phase-separated PS domains within a continuous PBA matrix, for samples which employed 0, 2, and 5 mol% DVB in the PBA seed particle. The mechanical properties of these films were those of a soft thermoplastic. After annealing above the polystyrene T_g, the modulus, fracture stress, and fracture energy increased significantly. These changes, and the development of yielding and stress-whitening phenomena, were attributed to an interconnected PS phase, possibly semi- or co-continuous with the PBA phase. This thermally

induced coalescence of the previously dispersed PS phase was also evident from dynamic mechanical studies. The level of crosslinking within the seed was shown to affect the morphology of both as-dried and annealed films, as judged from the mechanically effective volume fraction of PS within the PBA matrix. The effects of higher seed crosslinking, larger seed particle size, and higher total styrene content were to increase the relative amount of PS at the two-stage particle surfaces, resulting in poor film formation at room temperature. Annealing of these materials led to a more continuous PS phase and mechanical properties similar to those of rubber-modified polystyrene.

The authors gratefully acknowledge the assistance of R. B. Olson, M. Lo, and A. Pinero for obtaining DMA, particle size and residual monomer data, respectively. The authors also thank Professor F. Karasz for helpful discussions and Ms. Sandy Determan for typing the manuscript.

References

1. C. B. Bucknall, "*Toughened Plastics*," Applied Science Publishers, London, 1977, Chapter 4.

2. J. C. Daniels, *Makromol. Chem., Suppl.* **10/11**, 359 (1985).

3. A. Guyot, J. Guillot, C. Pichot, and L. Rios Guerrero, in *Emulsion Polymers and Emulsion Polymerization*, D. R. Bassett and A. E. Hamielec, Eds., ACS Symposium Series #165, 1981, p. 415.

4. S. Nishida, M. S. El-Assar, A. Klein, and J. W. Vanderhoff, in *Emulsion Polymers and Emulsion Polymerization*, D. R. Bassett and A. E. Hamielec, Eds., ACS Symposium Series #165, 1981, p. 291.

5. M. Okubo, Y. Katsuta, and T. Matsumoto, *J. Polym. Sci., Polym. Lett. Ed.*, **18**, 481 (1980); **20**, 45 (1982).

6. T. J. Min, A. Klein, M. S. El-Assar, and J. W. Vanderhoff, *J. Polym. Sci., Chem. Ed.*, **21**, 2845 (1983).

7. D. R. Bassett and K. L. Hoy, in *Emulsion Polymers and Emulsion Polymerization*, D. R. Bassett and A. E. Hamielec, Eds., ACS Symposium Series #165, 1981, p. 371.

8. I. Cho and K. W. Lee, *J. Appl. Polym. Sci.*, **30**, 1903 (1985).

9. M. Chainey, J. Hearn, and M. C. Wilkinson, *Br. Polym. J.*, **13**, 132 (1981).

10. M. Okubo, M. Ando, A. Yamada, Y. Katsuta, and T. Matsumoto, *J. Polym. Sci., Polym. Lett. Ed.*, **19**, 143 (1981).

11. J. R. Erickson and R. J. Seidewand, in *Emulsion Polymers and Emulsion Polymerization*, D. R. Bassett and A. E. Hamielec, Eds., ACS Symposium Series #165, 1981, p. 483.

12. T. Matsumoto, M. Okubo, and S. Shibao, *Kobunshi Ronbunshu*, **33**, 575 (1976).

13. M. Okubo, Y. Katsuta, A. Yamada, and T. Matsumoto, *Kobunshi Ronbunshu*, **36**, 459 (1979).

14. A. Okubo, A. Yamada, and T. Matsumoto, *J. Polym. Sci., Polym. Chem. Ed.*, **16**, 3219 (1980).

15. S. Muroi, H. Hashimoto, and K. Hosoi, *J. Polym. Sci., Polym. Chem. Ed.*, **22**, 1365 (1984).

16. R. L. Rowell, J. R. Ford, J. W. Parsons, and D. R. Bassett, in *Polymer Colloids II*, R. M. Fitch, Ed., Plenum, New York, 1980, p. 27.

17. R. A. Dickie, M. F. Cheung, and S. Newman, *J. Appl. Polym. Sci.*, **17**, 65 (1973).

18. R. A. Dickie and M. F. Cheung, *J. Appl. Polym. Sci.*, **17**, 70 (1973).

19. S. C. Misra, C. Pichot, M. S. El-Assar, and J. W. Vanderhoff, *J. Polym. Sci., Polym. Chem. Ed.*, **21**, 2383 (1983).

20. L. H. Sperling, T. W. Chiu, and D. A. Thomas, *J. Appl. Polym. Sci.*, **17**, 2443 (1973).

21. M. Okubo, M. Seike, and T. Matsumoto, *J. Appl. Polym. Sci.*, **28**, 383 (1983).

22. P. N. Pusey, in *Colloid Dispersions*, J. W. Goodwin, Ed., Henry Lind Ltd., Dorchester, Dorset, Great Britain, 1982, Chapter 6.

23. J. W. Vanderhoff, H. L. Tarkowski, M. C. Jenkins, and E. B. Bradford, *Rubber Chem. Technol.*, **40**, 1246 (1967).

24. O. Olabisi, L. M. Robeson, and M. T. Shaw, *Polymer-Polymer Miscibility*, Academic Press, New York, 1979, Chapter 3.

25. A. Weitz and B. Wunderlich, *J. Polym. Sci., Polym. Phys. Ed.*, **12**, 2473 (1974).

26. W. J. MacKnight, F. E. Karasz, and J. R. Fried, in *Polymer Blends*, D. R. Paul and S. Newman, Eds., Academic Press, New York, 1978, Vol. 1, Chapter 5.

27. A. R. Berens and H. B. Hopfenberg, *J. Membrane Sci.*, **10**, 283 (1982).

28. J. Crank and G. S. Park, Eds., *Diffusion in Polymers*, Academic Press, London, 1968.

29. T. G. Fox and P. J. Flory, *J. Polym. Sci.*, **14**, 315 (1954).

30. J. F. Beecher, L. Marker, R. D. Bradford, and S. L. Aggarwal, *J. Polym. Sci., Part C*, **26** 117 (1969).

Received April 3, 1986
Accepted October 14, 1986